JOURNAL OF MATERIALS SCIENCE 21 (1986) 1693–1699

Resistometric study on kinetics of reversible short-range ordering and crossover effect in $Fe_{15}Ni_{63}Si_8B_{14}$ metallic glass

T. KOMATSU, K. MATUSITA
Department of Materials Science and Technology, Technological University of Nagaoka, Nagaoka, 949–54 Japan

The kinetics of reversible short-range ordering (SRO) and crossover effect in the fully stabilized $Fe_{15}Ni_{63}Si_8B_{14}$ metallic glass were examined by measurements of electrical resistivity change. The kinetic parameters for reversible SRO in the narrow temperature range from 240 to 280° C were determined to be 1.93 eV for the activation energy, 8.6×10^{-16} sec for the pre-exponential factor and 2.3 for the width of the distribution of relaxation times on the assumption of a log-normal distribution. The crossover effect in reversible short-range ordering and disordering was clearly observed.

1. Introduction

Metallic glasses prepared by various rapid-quenching techniques are thermodynamically unstable and tend to relax toward more stable structure during annealing well below the glass transition temperature without crystallization. Since structural relaxation affects various physical, chemical and mechanical properties, it is quite important to clarify the relaxation phenomenon in metallic glasses not only for technical applications but also for understanding the glass structure. Structural relaxation in Fe–Ni based ferromagnetic metallic glasses has been extensively studied by various measurements such as those of density [1–3], electrical resistivity [4–11], Curie temperature [12–14], induced magnetic anisotropy [15], elastic modulus [16, 17] and internal friction [18], and it has been proposed that two types of short-range ordering (SRO), namely irreversible (topological) and reversible (compositional), occur during structural relaxation. The crossover effect is also an important phenomenon in the structural relaxation of amorphous materials and has been observed in the changes in Curie temperature [19–22] and elastic modulus [16, 23] of metallic glasses. However, the mechanism of structural relaxation is not well clarified at the present time and more extensive studies, particularly compositional dependence, kinetics, crossover effect and correlations among the various properties, are desired. The purpose of the present study is to examine the kinetics of reversible SRO and crossover effect in $Fe_{15}Ni_{63}Si_8B_{14}$ metallic glass by measurements of changes in electrical resistivity during structural relaxation.

2. Experimental procedure

An $Fe_{15}Ni_{63}Si_8B_{14}$ metallic glass was prepared in the form of a ribbon, 20 μm thick and 1.37 mm wide, by rapid quenching using a single-roller casting apparatus. The amorphous state was confirmed by X-ray diffraction. The measurements of electrical resistivity were made using a four-point probe method. As-quenched samples were spot-welded carefully by small copper wires. The samples were annealed in a furnace at a constant temperature. During annealing nitrogen or argon gas was flowed to prevent an oxidation of samples. After each predetermined time interval, the annealing was interrupted and the samples were quenched in acetone to room temperature. The samples were then immersed in liquid nitrogen (77 K) to measure the electrical resistivity.

3. Results and discussion

3.1. Pre-annealing of $Fe_{15}Ni_{63}Si_8B_{14}$ metallic glass

It is well known that in as-quenched Fe–Ni based metallic glasses both irreversible and reversible SRO occur during structural relaxation, while in pre-annealed (stabilized) metallic glasses which were annealed near the glass transition temperature (T_g) or below the crystallization temperature (T_x), almost only reversible SRO occurs by annealing at temperatures below the pre-annealing temperature. Therefore, for the study of reversible SRO, $Fe_{15}Ni_{63}Si_8B_{14}$ metallic glass must be first stabilized by annealing near T_g or below T_x without causing any crystallization.

The crystallization behaviour in $Fe_{15}Ni_{63}Si_8B_{14}$ metallic glass was examined by thermal expansion measurements and a differential scanning calorimetry (DSC), and a typical thermal expansion curve is shown in Fig. 1. The crystallization temperatures (T_x) determined from the thermal expansion curves are plotted in Fig. 2 as a function of heating rate. Fig. 2 indicates that the crystallization would occur after a long time annealing around 400° C. The resistivity changes ($\Delta\varrho/\varrho$) caused by isochronal annealing in the as-quenched sample were measured (Fig. 3). As can be seen in Fig. 3, the resistivity increases with increasing the annealing temperature up to 375° C and then

0022–2461/86 $03.00 + .12

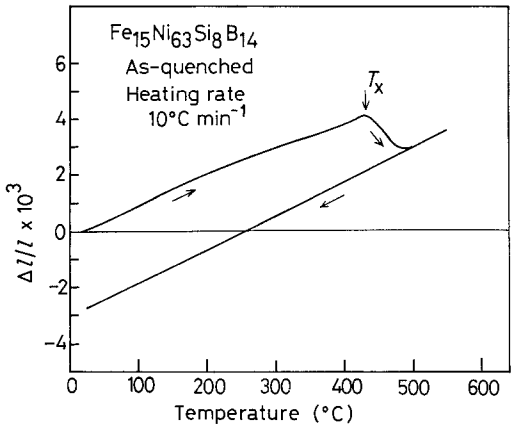

Figure 1 Thermal expansion curve of as-quenched $Fe_{15}Ni_{63}Si_8B_{14}$ metallic glass. Heating rate was 10° C min^{-1}.

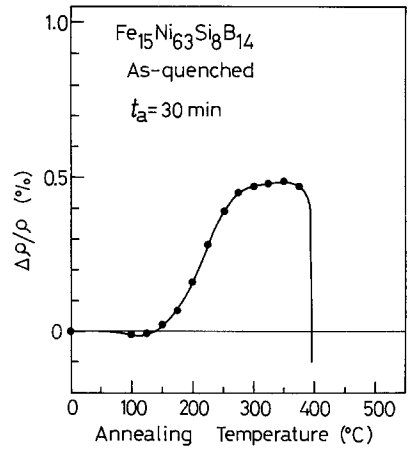

Figure 3 Resistivity changes ($\Delta\varrho/\varrho$) caused by isochronal annealing in the as-quenched $Fe_{15}Ni_{63}Si_8B_{14}$ metallic glass. Annealing time (t_a) was 30 min.

decreases rapidly due to the crystallization. These results (Figs. 1 to 3) indicate clearly that the pre-annealing temperature must be below 375° C.

The resistivity changes caused by isothermal annealing at 350 and 375° C were shown in Fig. 4. As can be seen in Fig. 4, the equilibrium resistivity change was not obtained in a proper annealing time at 350° C and the resistivity decreases after 1 h annealing at 375° C, maybe due to the onset of crystallization. Thus, after annealing at 375° C for 30 min, the sample was again annealed isothermally at 350° C (Fig. 5). As can be seen in Fig. 5, the resistivity changes became constant for annealing times of more than 20 min. From these results (Figs. 4 and 5), conditions of pre-annealing temperature and time for the stabilization of $Fe_{15}Ni_{63}Si_8B_{14}$ metallic glass was determined as follows; first annealing at 375° C for 30 min and second annealing at 350° C for 30 min. Since these annealing temperatures (375 and 350° C) are not far below T_x and no crystallization occurs, it is considered that these pre-annealing temperatures and times are adequate for the stabilization of $Fe_{15}Ni_{63}Si_8B_{14}$ metallic glass. The samples stabilized by the above annealing method were used for the study of kinetics of reversible SRO and crossover effect.

3.2. Reversible SRO

Before studying the kinetics of reversible SRO and crossover effect in $Fe_{15}Ni_{63}Si_8B_{14}$ metallic glass, it must be guaranteed that only reversible SRO occurs in the stabilized samples. The resistivity changes caused by isochronal annealing (from 100 to 345° C) in the stabilized $Fe_{15}Ni_{63}Si_8B_{14}$ metallic glass are shown in Fig. 6. The resistivity changes caused by isochronal annealing cycles, in which the stabilized samples were annealed at decreased temperatures (from 330 to 250° C) and then the samples were again annealed at increased temperatures (from 260 to 340° C), are shown in Fig. 7. The resistivity changes caused by isothermal annealing in the stabilized samples are shown in Fig. 8. These results indicate that, in the high-temperature region above 300° C, an equilibrium state for the resistivity change is achieved very rapidly by annealing, while in the low-temperature region below 300° C, it is necessary to anneal the samples for a very long time for the establishment of the equilibrium state. The equilibrium values of resistivity change in isochronal (Figs. 6 and 7) and isothermal (Fig. 8) annealings are plotted in Fig. 9 as a function of annealing temperature. As can be seen in Fig. 9, the equilibrium values of resistivity change lie on the same straight line for the annealing temperature, and its line intercepts the annealing temperature of 350° C which is used for the stabilization of $Fe_{15}Ni_{63}Si_8B_{14}$ metallic glass. These results inicate that only reversible resistivity changes occur during various annealings (annealing temperatures are below the pre-annealing temperature 350° C) in the stabilized samples and the equilibrium

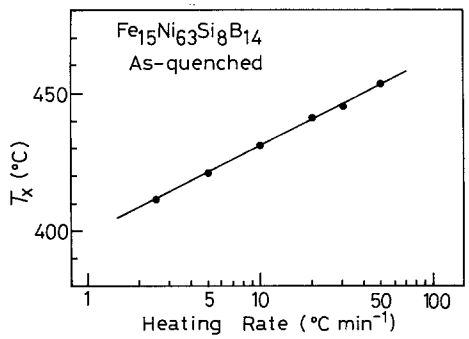

Figure 2 Crystallization temperature (T_x) of as-quenched $Fe_{15}Ni_{63}Si_8B_{14}$ metallic glass as a function of heating rate. T_x was determined from the thermal expansion curve.

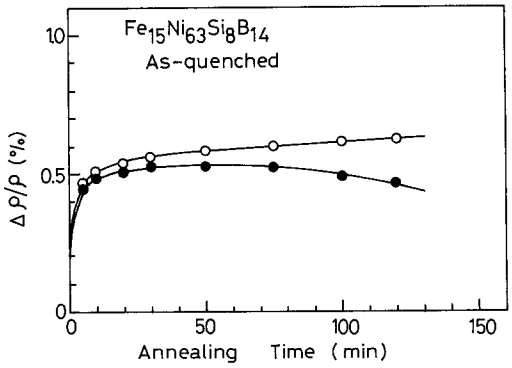

Figure 4 Resistivity changes ($\Delta\varrho/\varrho$) caused by isothermal annealing (T_a) at (○) 350 and (●) 375° C in the as-quenched $Fe_{15}Ni_{63}Si_8B_{14}$ metallic glass.

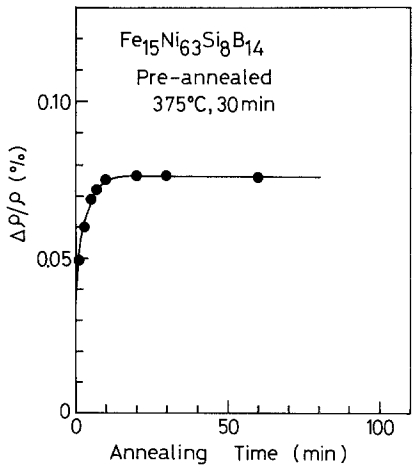

Figure 5 Resistivity changes ($\Delta\varrho/\varrho$) caused by isothermal annealing at 350° C in the pre-annealed $Fe_{15}Ni_{63}Si_8B_{14}$ metallic glass.

values of resistivity changes are independent of the direction of approach to equilibrium.

Electrical resistivity measurements have been used extensively for the study of structural relaxation of metallic glasses and the reversibility in the resistivity change similar to the present results has been reported in Fe–Ni based glass and another metallic glass. Balanzat *et al.* [5] have shown that a reversible resistivity change during structural relaxation in $Fe_{40}Ni_{40}P_{14}B_6$ metallic glass is due to the compositional SRO between iron and nickel atoms. Recently, Komatsu *et al.* [8, 11] reported that the reversible resistivity change during structural relaxation in $(Fe_xNi_{1-x})_{78}Si_8B_{14}$ metallic glasses is largely affected by the Fe/Ni ratio and found an almost linear correlation between the reversible changes in resistivity and Curie temperature in the pre-annealed $Fe_{27}Ni_{53}P_{14}B_6$ metallic glass. Similar reversibilities have been observed in various other physical properties and are generally attributed to reversible SRO. From the above, it is considered that the reversible resistivity change in the stabilized $Fe_{15}Ni_{63}Si_8B_{14}$ metallic glass corresponds to the reversible changes in the short-range structure. As a conclusion, the results shown in Figs. 6 to 9 indicate that only reversible SRO can be reproduced in the stabilized $Fe_{15}Ni_{63}Si_8B_{14}$ metallic glass, depending on the annealing temperature. Since the Curie temperature of as-quenched $Fe_{15}Ni_{63}Si_8B_{14}$ metallic glass is 253 K and is far below the annealing temperatures, it is considered that the kinetics of reversible SRO are not affected by the magnetic energy.

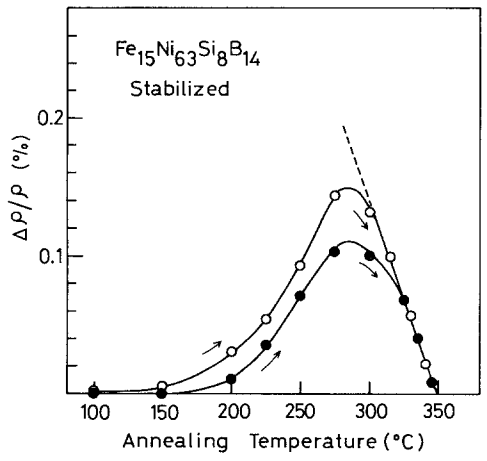

Figure 6 Resistivity changes ($\Delta\varrho/\varrho$) caused by isochronal annealing in the stabilized $Fe_{15}Ni_{63}Si_8B_{14}$ metallic glass. Annealing times (t_a) were (●) 10 and (○) 60 min.

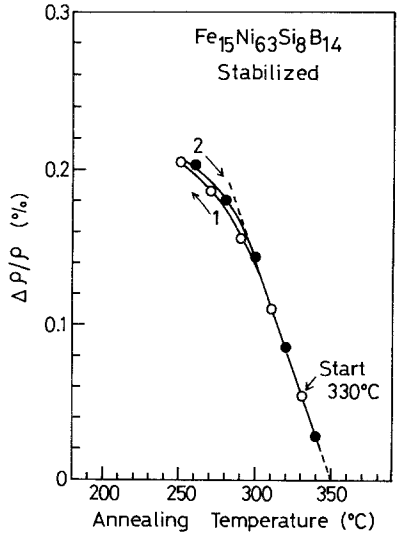

Figure 7 Resistivity changes ($\Delta\varrho/\varrho$) caused by isochronal annealing cycles in the stabilized $Fe_{15}Ni_{63}Si_8B_{14}$ metallic glass. Annealing time (t_a) was 30 min. (○) First run, decreasing, (●) second run, increasing.

3.3. Kinetics of reversible SRO

The relaxation of various properties in amorphous materials is generally not described by a single relaxation time in the temperature range near and below the glass transition [24]. It is often convenient to describe the relaxation process of amorphous materials in terms of the distribution of relaxation times (a log-normal distribution) [24, 25]. In this structural relaxation model, the relaxation function, $\psi(T, t)$, can be expressed as

$$\frac{P(T, t) - P_\infty}{P_0 - P_\infty} = \psi(T, t) = \exp\{-[t/\tau(T)]^{1/\beta}\} \quad (1)$$

$$\tau(T) = \tau_0 \exp(\Delta E_a/k_B T) \quad (2)$$

where P_0 and P_∞ are the initial and equilibrium physical properties in the amorphous materials, $\tau(T)$ is the

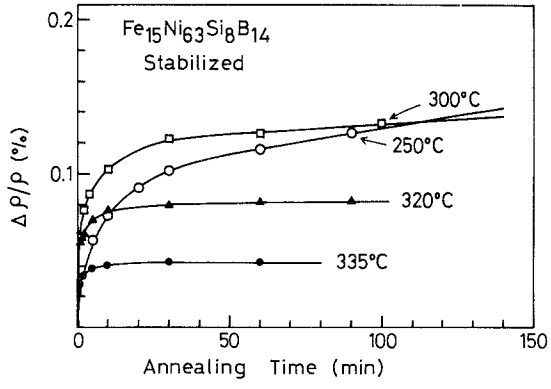

Figure 8 Resistivity changes ($\Delta\varrho/\varrho$) caused by isothermal annealing at 250, 300, 320 and 335° C in the stabilized $Fe_{15}Ni_{63}Si_8B_{14}$ metallic glass.

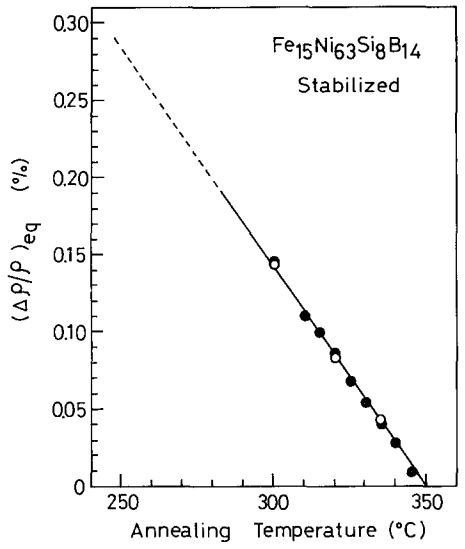

Figure 9 Equilibrium values $(\Delta\varrho/\varrho)_{eq}$ in the resistivity changes caused by (●) isochronal and (○) isothermal annealings in the stabilized $Fe_{15}Ni_{63}Si_8B_{14}$ metallic glass.

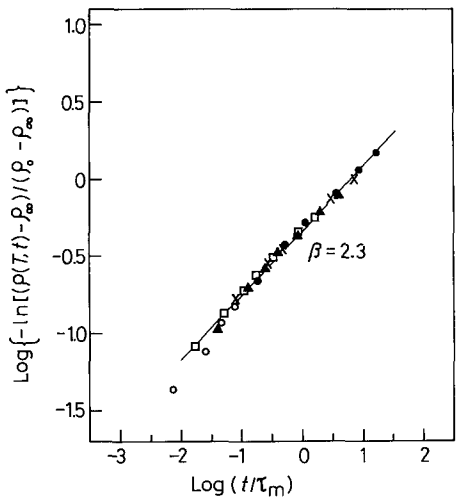

Figure 11 Normalized resistivity changes as a function of log (t/τ_m) in the stabilized $Fe_{15}Ni_{63}Si_8B_{14}$ metallic glass. T_a values of (○) 240° C, (□) 250° C, (▲) 260° C, (×) 270° C, (●) 280° C.

relaxation time, τ_0 is the pre-exponential factor, β is the relaxation function constant and means the width of the distribution of relaxation times, ΔE_a is the activation energy of the relaxation process and k_B is the Boltzmann constant.

The resistivity changes caused by isothermal annealing at various temperatures (240, 250, 260, 270 and 280° C) below the pre-annealing temperature in the stabilized $Fe_{15}Ni_{63}Si_8B_{14}$ metallic glass were measured (Fig. 10). Assuming that the equilibrium values of resistivity changes at these low temperatures are obtained by extrapolating the values at high temperatures in Fig. 9, the kinetics of reversible resistivity changes was analysed using Equations 1 and 2. In this analysis, the relaxation time $\tau(T)$ corresponds to the mean characteristic relaxation time which is equal to the time at $(\Delta\varrho/\varrho)/(\Delta\varrho/\varrho)_{eq} = 1/e$. The results are shown in Figs. 11 and 12. It is clear that the relaxation curve for the reversible resistivity changes at the different annealing temperatures can be brought into almost a single master curve and the mean characteristic relaxation time obeys an Arrhenius law. The kinetic parameters for the reversible resistivity changes in the stabilized $Fe_{15}Ni_{63}Si_8B_{14}$ metallic glass were derived as follows. The value of β is 2.3, the activation energy ΔE_a 1.93 eV and τ_0 8.6 $\times$ 10^{-16} sec.

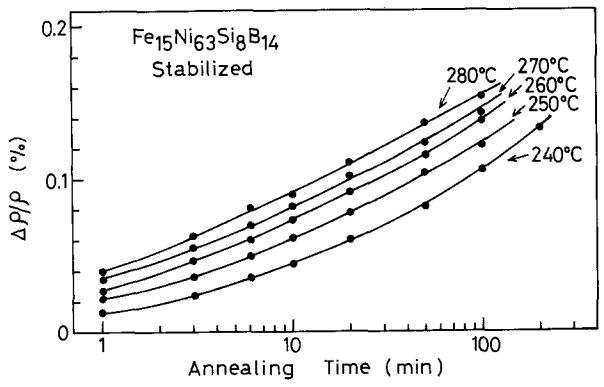

Figure 10 Resistivity changes $(\Delta\varrho/\varrho)$ caused by isothermal annealing in the stabilized $Fe_{15}Ni_{63}Si_8B_{14}$ metallic glass.

The kinetic parameters (β, ΔE_a, τ_0) for reversible relaxation in other Fe–Ni and Co-based metallic glasses have been reported and are summarized in Table I. The values of $\beta = 2.3$ obtained in the stabilized $Fe_{15}Ni_{63}Si_8B_{14}$ metallic glass coincides with the values in $Fe_{40}Ni_{40}B_{20}$ ($\beta = 2.5$) [16] and (Co, Fe, $Ni)_{73}(Si, B)_{27}$ ($\beta = 2.5$) [9] metallic glasses but differs from the values in $Fe_{40}Ni_{40}P_{14}B_6$ ($\beta = 4$) [4, 15] and $(Co, Fe)_{75}Si_{15}B_{10}$ ($\beta = 5$) [26] metallic glasses. It is to be noted that the value of $\beta = 2.3$ obtained in the present study is almost same as the value of $\beta = 2.2$ for the relaxation of oxide glass below the glass transition temperature [25]. The activation energy and pre-exponential factor in the stabilized $Fe_{15}Ni_{63}Si_8B_{14}$ metallic glass are approximately similar to the values in other Fe–Ni and Co-based metallic glasses. The data on activation energies (Q) for diffusion of some elements in Fe–Ni based metallic glasses are shown in Table II. It is obvious that the value of activation energy for reversible SRO in the stabilized $Fe_{15}Ni_{63}Si_8B_{14}$ metallic glass is smaller than those for diffusion of metalloid atoms (phosphorus, boron, silicon) and is close to the activation energy for diffusion

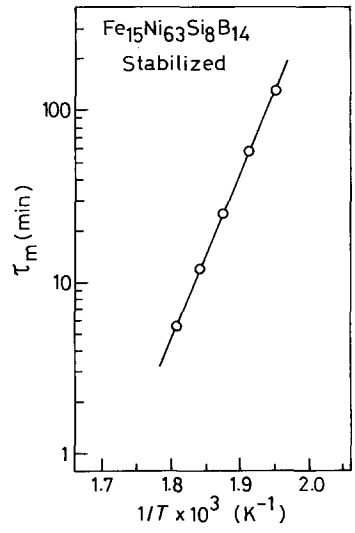

Figure 12 Arrhenius plot of the mean characteristic relaxation time (τ_m). $\Delta E_a = 1.93$ eV.

TABLE 1 Kinetic parameters for reversible structural relaxation in Fe–Ni and Co-based metallic glasses. β is the width of the distribution of relaxation times, ΔE_a is the activation energy and τ_0 is the pre-exponential fator

Composition	β	ΔE_a (eV)	τ_0 (sec)	Method*	Reference
$Fe_{15}Ni_{63}Si_8B_{14}$	2.3	1.93	8.6×10^{-16}	a	This work
$Fe_{40}Ni_{40}P_{14}B_6$	4	1.63	10^{-14}	a	[4]
	4	1.74	6.7×10^{-16}	b	[15]
$Fe_{40}Ni_{40}B_{20}$	2.5	1.76		c	[16]
$(Co, Fe, Ni)_{73}(Si, B)_{27}$	2.5	1.82	5.5×10^{-14}	a	[9]
$(Co, Fe)_{75}Si_{15}B_{10}$	5	2.0	7.8×10^{-17}	b	[26]
$Co_{58}Ni_{10}Fe_5Si_{11}B_{16}$		1.8 ~ 2.3	6×10^{-16}	b	[27]
		1.85	5×10^{-16}	b	[28]

*a, resistivity, b, induced magnetic anisotropy; c, Young's modulus.

of iron atoms. These results may indicate that reversible SRO in $Fe_{15}Ni_{63}Si_8B_{14}$ metallic glass is largely related to mobilities of iron and nickel atoms. It is to be pointed out that the value of the frequency factor ($\nu_0 = 10^{15}\,sec^{-1}$, $\nu_0 = 1/\tau_0$) in the stabilized $Fe_{15}Ni_{63}Si_8B_{14}$ metallic glass is much larger than the characteristic Debye frequency factor ($\nu_0 = 10^{13}\,sec^{-1}$). This may relate to open structure with smaller density [3] and smaller Debye temperature [34] in metallic glasses.

3.4. Crossover effect in reversible SRO

The crossover effect was examined in the stabilized $Fe_{15}Ni_{63}Si_8B_{14}$ metallic glass and the results are shown in Fig. 13. In these experiments, the relationship between the annealing temperature and the equilibrium value of resistivity change (Fig. 9) was used. In the crossover experiments for short-range ordering (curve a, Fig. 13), the stabilized sample was annealed at 340° C (T_0) until the resistivity change ($\Delta\varrho/\varrho$) became an equilibrium value, then the sample was annealed at 300° C (T_1) for 1 min and the resistivity change in this sample corresponds to the equilibrium resistivity change at the annealing temperature of 317° C. Thus, the sample annealed at 300° C for 1 min was again annealed isothermally at 317° C (T_2). Similar experimental procedures were used for short-range disordering (curve b, Fig. 13). As can be seen in Fig. 13, it is obvious that the crossover effect is clearly observed in both short-range ordering ($T_0 > T_2 > T_1$) and disordering ($T_0 < T_2 < T_1$). The crossover effect for short-range ordering at various T_2 ($T_1 = 250°$ C) is shown in Fig. 14. It is found that the amount of crossover, $(\Delta\varrho/\varrho)_{cr}$, which corresponds to the departure of resistivity change from the equilibrium, depends greatly on the thermal history. The values of $(\Delta\varrho/\varrho)_{cr}$ are plotted in Fig. 15 as a function of T_2. The results indicate that the linear relationship is found between the values of $(\Delta\varrho/\varrho)_{cr}$ and T_2 and its line intercepts at the initial (e.g. stabilized) annealing temperature ($T_0 = 350°$ C). The above results indicate that even if the values of resistivity change are the same, short-range structure differs depending on the annealing temperature. In other words, the relaxation mechanism for reversible SRO in the stabilized $Fe_{15}Ni_{63}Si_8B_{14}$ metallic glass cannot be explained by a single ordering parameter.

TABLE II Activation energies (Q) for diffusion in Fe–Ni based metallic glasses

Composition	Diffusion species	Q (eV)	Reference
$Fe_{40}Ni_{40}P_{14}B_6$	Fe	2.0	[29]
	P	3.1	[30]
$Fe_{40}Ni_{40}B_{20}$	B	3.6	[31]
$Fe_{32}Ni_{36}Cr_{14}P_{12}B_6$	P	1.8	[32]
$Fe_{82}Si_6B_{12}$	Si	2.8	[33]

The crossover effect is a well-known phenomenon in the structural relaxation in borate and borosilicate oxide glasses [35, 36] and is still one of the important subjects concerning the relaxation mechanism. Even in the metallic glasses, the crossover effect has been observed in the physical properties such as Curie temperature [19–22] and elastic modulus [15, 23]. In some metallic glasses [16, 19], the crossover effect has been analysed successfully in terms of a two-relaxation time model, even though it would be more reasonable to interpret the crossover effect in terms of the distribution of relaxation times, as described in the analysis of the kinetic parameters for reversible SRO. When the stabilized sample was annealed at a low temperature ($T_1 = 250°$ C) in Fig. 14, it is considered that reversible SRO with short relaxation times occurs rapidly and reversible SRO with longer relaxation times proceeds slowly. If the annealing at T_1 is interrupted and the sample is annealed at higher temperature ($T_2 = 313$, 324 or 334° C), disordering (decrease in the resistivity) with short relaxation times

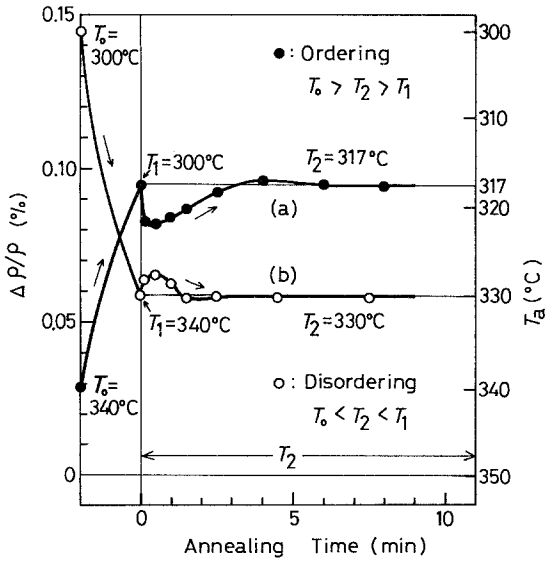

Figure 13 Crossover effect in the short-range ordering (curve a) and disordering (curve b) in the stabilized $Fe_{15}Ni_{63}Si_8B_{14}$ metallic glass. Experimental procedures are described in the text.

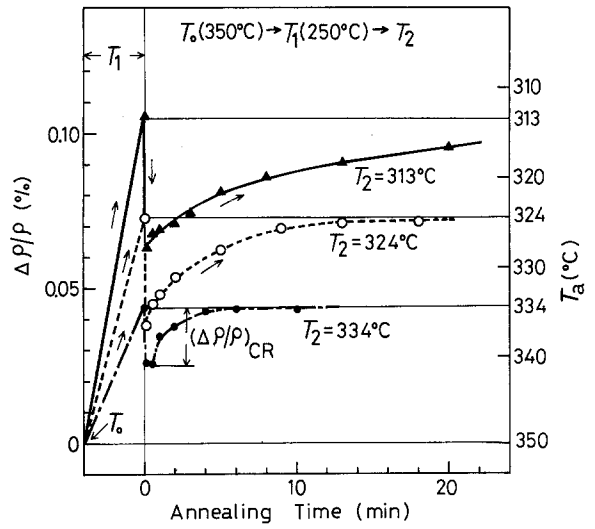

Figure 14 Crossover effect in the short-range ordering in the stabilized $Fe_{15}Ni_{63}Si_8B_{14}$ metallic glass.

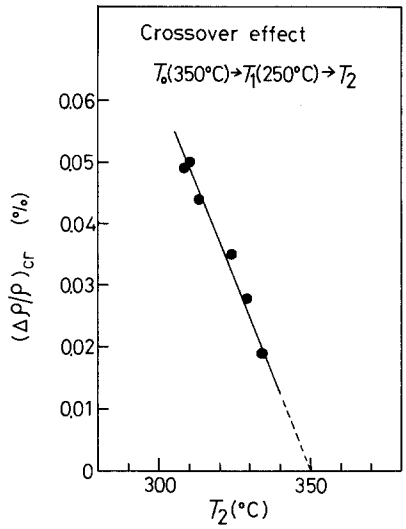

Figure 15 The values of $(\Delta\varrho/\varrho)_{cr}$ in the crossover experiments in the stabilized $Fe_{15}Ni_{63}Si_8B_{14}$ metallic glass.

occurs together with ordering with longer relaxation times approaching the equilibrium short-range ordered structure at T_2. Therefore the recovery of resistivity change can be observed as shown in Fig. 14.

3.5. The short-range ordered structure

It is very important to clarify short-range ordered structure which changes reversibly in metallic glasses. Recently, Komatsu *et al.* [3] measured volume changes (e.g. density changes) by annealing in $(Fe_xNi_{1-x})_{78}Si_8B_{14}$ metallic glasses and found that the volume changes due to the structural relaxation and crystallization depend greatly on the Fe/Ni ratio, being minimum at the composition $Fe_{15}Ni_{63}Si_8B_{14}$. Considering that the "Ni_3Fe" phase exists in the Fe–Ni crystalline alloy system, Komatsu *et al.* suggested from those results that a highly ordered short-range structure such as "Ni_3Fe" of $(Ni_{0.75}Fe_{0.25})_3$(Si, B) trigonal prism is already formed in the as-quenched $Fe_{15}Ni_{63}Si_8B_{14}$ metallic glass. From various studies [37–41], it is considered that at least in transition metal (TM)–metalloid (M) metallic glasses around $TM_{75}M_{25}$ composition a basic structural unit is a trigonal prism such as (Fe, Ni)$_3$B. Eickelman *et al.* [41] examined the local structure in $(Ni_{0.75}Fe_{0.25})_{75}B_{25}$ metallic glass by Mössbauer effect and suggested that the local structure in the glassy sample is similar to that in the crystalline sample. From the above, short-range structure based on the $(Ni_{0.75}Fe_{0.25})_3$(Si, B) trigonal prism might be a suitable unit for the structure which changes reversibly in the stabilized $Fe_{15}Ni_{63}Si_8B_{14}$ metallic glass. In this structure model, reversible SRO with short relaxation times would correspond to movements of iron and nickel atoms in the trigonal prism and reversible SRO with long relaxation times would correspond to rearrangements of trigonal prisms.

Recently, Balanzat and Hillairet [42] examined short-range ordering in $Cu_{50}Ti_{50}$ and $Ni_{35}Ti_{65}$ metallic glasses by resistivity measurements and suggest that ordered domains exist. Furthermore, it is to be noted that the reversibility and crossover effect in the resistivity change similar to those in metallic glasses have been observed in short-range ordering and disordering in a crystalline Cu(15 at %)–Al alloy by Trieb and Veith [43] and the results are interpreted by a heterogeneous model of SRO in which ordered regions are dispersed in a less ordered matrix, depending on temperature. The problem whether reversible SRO in metallic glasses occurs homogeneously or heterogeneously has not been solved and is very important for the understanding of structural relaxation. More extensive study on reversible SRO in metallic glasses is now in progress.

4. Conclusion

The annealing conditions for the stabilization of $Fe_{15}Ni_{63}Si_8B_{14}$ metallic glass were first determined and it was then confirmed from the measurements of resistivity change that only reversible short-range ordering (SRO) and disordering occur below the pre-annealing temperature in the stabilized samples. The kinetic parameters for reversible SRO in the narrow temperature range from 240 to 280° C were determined to be 1.93 eV for the activation energy, 8.6×10^{-16} sec for the pre-exponential factor, and 2.3 for the width of the distribution of relaxation times on the assumption of a log-normal distribution. The crossover effect in reversible short-range ordering and disordering was clearly observed.

References

1. H. H. LIEBERMANN, C. D. GRAHAM Jr and P. J. FLANDERS, *IEEE Trans. Mag.* **MAG-13** (1977) 1541.
2. A. KURŠUMOVIĆ, R. W. CAHN and M. G. SCOTT, *Scripta Metall.* **14** (1980) 1245.
3. T. KOMATSU, K. MATUSITA and R. YOKOTA, *J. Non-Cryst. Solids* **69** (1985) 347.
4. M. BALANZAT, *Scripta Metall.* **14** (1980) 173.
5. E. BALANZAT, C. MAIRY and J. HILLAIRET, *J. Physique* **C8** (1980) 871.
6. J. R. COST and J. T. STANLEY, *Scripta Metall.* **15** (1981) 407.
7. P. ALLIA, D. ANDREONE, R. SATO TURLELLI, F. VINAI and G. RIONTINO, *J. Appl. Phys.* **53** (1982) 8798.
8. T. KOMATSU, R. YOKOTA, T. SHINDO and K. MATSUITA, *J. Non-Cryst. Solids* **65** (1984) 63.
9. R. YOKOTA, M. TAKEUCHI, T. KOMATSU and K. MATUSITA, *J. Appl. Phys.* **55** (1984) 3037.
10. T. KOMATSU, K. MATUSITA and R. YOKOTA, *J.*

Mater. Sci. **20** (1985) 1375.
11. *Idem, ibid.* **20** (1985) 3271.
12. T. EGAMI, *Mat. Res. Bull.* **13** (1978) 557.
13. Y. N. CHEN and T. EGAMI, *J. Appl. Phys.* **50** (1979) 7615.
14. T. MIZOGUCHI, H. KATO, N. AKUTSU and S. HATTA, Proceedings of the 4th International Conference on Rapidly Quenched Metals, Sendai (1981) edited by T. Masumoto and K. Suzuki, Vol. 2 (Japan Institute of Metals, Sendai, 1982) p. 1173.
15. W. CHAMBRON and A. CHAMBEROD, *Solid State Commun.* **33** (1980) 157.
16. M. G. SCOTT and A. KURŠUMOVIĆ, *Acta Metall.* **30** (1982) 853.
17. A. VAN DEN BEUKEL, S. VAN DER ZWAAG and A. L. MULDER, *ibid.* **32** (1984) 1895.
18. N. MORITO and T. EGAMI, *ibid.* **32** (1984) 603.
19. A. L. GREER and J. A. LEAKE, *J. Non-Cryst. Solids* **33** (1979) 291.
20. H. S. CHEN, *J. Appl. Phys.* **52** (1981) 1868.
21. N. MORITO and T. EGAMI, *IEEE Trans. Mag.* **MAG-19** (1983) 1898.
22. J. A. LEAKE, M. R. J. GIBBS, S. VRYENHOEF and J. E. EVETTS, *J. Non-Cryst. Solids* **61/62** (1984) 787.
23. K. BOTHE and H. NEUHAUSER, *ibid.* **56** (1983) 279.
24. D. R. UHLMANN and R. W. HOPPER, "Metallic glasses", edited by J. J. Gilman and H. J. Leamy (American Society for Metals, Ohio, 1978) p. 218.
25. H. S. Y. HSICH, *J. Mater. Sci.* **15** (1980) 1194.
26. K. Y. HO, P. J. FLANDERS and C. D. GRAHAM Jr, *J. Appl. Phys.* **53** (1982) 2279.
27. H. Q. GUO, W. FERNENGEL, A. HOFMANN and H. KRONMÜLLER, *IEEE Trans. Mag.* **MAG-20** (1984) 1394.
28. W. CHAMBRON and A. CHAMBEROD, *J. Physique* **C5** (1981) 511.
29. P. VALENTA, K. MAIER, H. KRONMÜLLER and K. FREITAG, *Phys. Status Solidi (b)* **106** (1981) 129.
30. *Idem, ibid.* **105** (1981) 537.
31. R. W. CAHN, J. E. EVETTS, J. PATTERSON, R. E. SOMEKH and C. K. JACKSON *J. Mater. Sci.* **15** (1980) 702.
32. D. R. BAER, L. R. PEDERSON and M. T. THOMAS, *Mater. Sci. Eng.* **48** (1981) 283.
33. F. E. LUBORSKY and F. BACON, Proceeding of the 4th International Conference on Rapidly Quenched Metals, Sendai (1981), edited by T. Masumoto and K. Suzuki, Vol. 1 (Japan Institute of Metals, Sendai, 1982) p. 561.
34. D. G. ONN, "Amorphous Metallic Alloys", edited by F. E. Luborsky (Butterworths, London, 1983) p. 451.
35. L. BOESCH, A. NAPOLITANO and P. B. MACEDO, *J. Amer. Ceram. Soc.* **53** (1970) 148.
36. S. SPINNER and A. NAPOLITANO, *J. Res. Nat. Bur. Stand. Sec. A* **70** (1966) 147.
37. P. H. GASKELL, *J. Non-Cryst. Solids* **32** (1979) 207.
38. I. VINCZE and F. VAN DER WOUDE, *ibid.* **42** (1980) 499.
39. M. M. ABD-ELMEGUID, H. MICKLITZ and I. VINCZE, *Phys. Rev.* **B25** (1982) 1.
40. P. PANISSOD, I. BAKONYI and R. HASEGAWA, *ibid.* **B28** (1983) 2374.
41. H. J. EICKELMANN, M. M. ABD-ELMEGUID, H. MICKELITZ and R. A. BRAND, *ibid.* **B29** (1984) 2443.
42. E. BALANZAT and J. HILLAIRET, *J. Phys. F Met. Phys.* **12** (1982) 2907.
43. L. TRIEB and G. VEITH, *Acta Metall.* **26** (1978) 185.

Received 3 June
and accepted 9 July 1985